Multiscale modification of the conductive PEDOT:PSS polymer for the analysis of biological mixtures in a super-hydrophobic drop

Nicola Coppedè, Lorenzo Ferrara, Paolo Bifulco, Marco Villani, Salvatore Iannotta, Andrea Zappettini, Mario Cesarelli, Enzo Di Fabrizio, Francesco Gentile

PII: S0167-9317(16)30144-7
DOI: doi: 10.1016/j.mee.2016.03.033
Reference: MEE 10216

To appear in:

Received date: 21 October 2015
Revised date: 15 March 2016
Accepted date: 16 March 2016

Please cite this article as: Nicola Coppedè, Lorenzo Ferrara, Paolo Bifulco, Marco Villani, Salvatore Iannotta, Andrea Zappettini, Mario Cesarelli, Enzo Di Fabrizio, Francesco Gentile, Multiscale modification of the conductive PEDOT:PSS polymer for the analysis of biological mixtures in a super-hydrophobic drop, (2016), doi: 10.1016/j.mee.2016.03.033

Multiscale Modification of the Conductive PEDOT:PSS Polymer for the Analysis of Biological Mixtures in a Super-Hydrophobic Drop

Nicola Coppedè[1], Lorenzo Ferrara[2], Paolo Bifulco[3], Marco Villani[1], Salvatore Iannotta[1], Andrea Zappettini[1], Mario Cesarelli[3], Enzo Di Fabrizio[4,5], Francesco Gentile[3,5*]

[1] IMEM-CNR Parco Area delle Scienze 37/A - 43124 Parma, Italy,

[2] Istituto Italiano di Tecnologia, Via Morego 30, 16163 Genova, Italy

[3] Department of Electrical Engineering and Information Technology, University Federico II, Naples, Italy

[4] King Abdullah University of Science and Technology, Thuwal, Saudi Arabia

[5] Department of Experimental and Clinical Medicine, University of Magna Graecia, 88100 Catanzaro, Italy

* *corresponding author*: gentile@unicz.it, francesco.gentile2@unina.it

Conducting polymers are materials displaying high electrical conductivity, easy of fabrication, flexibility and biocompatibility, for this, they are routinely employed in organic electronics, printed electronics, and bioelectronics. Organic electrochemical transistors (OECTs) are a second generation of Organic Thin Transistors, in which the insulator layer is an electrolyte medium and the conductive polymer is electrochemically active. OECT devices have been demonstrated in chemical and biological sensing: while accurate in determining the size of individual ions in solution, similar devices break down if challenged with complex mixtures. Here, we combine a conductive PEODOT:PSS polymer with a super-hydrophobic scheme to obtain a family of advanced devices, in which the ability to manipulate a biological solution couples to a precise texture of the substrate (which incorporates five micro-electrodes in a line, and each is a site specific measurement point), and this permits to realize time and space resolved analysis of a solution. While the competition between convection and diffusion in a super-hydrophobic drop operates the separation of different species based on their size and charge, the described device delivers the ability to register a similar difference. In the following, we demonstrate the device in the sensing of a solution in which CTAB and adrenaline are separated with good sensitivity, selectivity and reliability.

Keywords: PEDOT:PSS, OECT, Super-hydrophobic surfaces, Biological mixtures, multiscale texture, Detection

1 Introduction

PEDOT:PSS is a conductive polymer that can be integrated into last generation Organic Electrochemical Transistor (OECT) devices for biological inspection, identification and analysis [1-3]. This material is a heavily doped p-type organic semiconductor, in which holes on the PEDOT chains (the semiconductor) are compensated by sulfonate anions on the PSS (the dopant). The application of a positive bias on a gate electrode immersed in the electrolyte causes cation injection into the PEDOT:PSS film. These cations compensate the sulfonate anions and dedope the PEDOT, thereby decreasing the drained current[4]. OECTs display bio compatibility, ease of integration into mechanically flexible substrates, high signal to noise ratio [1-2,5]: for this, they are routinely employed in biological applications, including bio-sensing, bio-interfacing and bio electronics [4, 6-9]. As regarding chemical and biological sensing, a variety of reports in literature demonstrated OECT devices in the recognition of individual species in a solution [5, 10-12], still their ability in resolving complex mixtures remains controversial.

Charge transport in OECTs has been firstly described by Bernards [13] with a model in which the response of the system is given by the combination of ionic transport in the electrolyte and hole transport in the conducting PEDOT:PSS. While efficacious in relating the time evolution of the current to the geometrical and physical characteristics of the PEDOT channel, the described model neglects size and charge effects of the ions in the electrolyte, thus it is impractical for detection.

In [14], it has been presented a mathematical model that relates the output of an OECT device to the diffusion coefficient (and thus the size) of charged species dispersed in the electrolyte of the device. The transportation of active species in the medium and thus the time of flight (TOF) from an initial position in the electrolyte to the PEDOT:PSS sensing surface would depend on size and charge of the described species. The TOF, in turn, and the velocity of charge accumulation on the PEDOT surface would determine the time-evolution of the current measured by the OCET device. In comparing experimental results of a real OECT device with the model, four different species individually placed in a solution were correctly identified. While accurate in determining the diffusion coefficient of individual ions in solution, the described method breaks downs if challenged with complex mixtures.

Here, we present a more sophisticated evolution of the method. We modified a conductive PEDOT:PSS polymer to include extra non-continuous scales in the device. This comprises super-hydrophobic SU8

pillars positioned on the substrate to form a non-periodic square lattice, in which the distance between the pillars smoothly transitions from the center to the periphery of the pattern [15]. The described non-periodic tiling generates a system of radial forces that recalls the drop to the center of the lattice [15]. The pattern incorporates a finite number of micro-electrodes in a line that represent the active or sensitive spots of the device (Figure 1). The entire system is coated in cascade with a conductive PEDOT:PSS polymer and by a fluorocarbon polymer (C_4F_8) which assures the hydrophobicity of the device [16]. A solution on a similar device would maintain a spherical shape as suspended in air [5, 17, 18]. Due to its curvature, Marangoni convective flows develop within the volume of a drop of solution [19-21]. The competition between convection and diffusion will cause a spatial separation of biological species that would depend on the size and charge of the species in a solution. On realizing a time and space resolved measurement of the solution, the described OECT device may operate the identification and separation of different species mingled up in a solution with high sensitivity, selectivity and reliability. The described method extends and completes the design proposed in [5], where super-hydrophobic PEDOT:PSS pillars are demonstrated without the integration of space-resolved measurement points.

2 Materials and Methods

Fabrication of the devices. Devices sensitive to charged species in a solution were designed and micro fabricated. The devices are given by the superposition and correct alignment of different layers. Layer A, that is a silicon substrate which contains conductive gold circuits connecting the electric active areas in the interior of the device, to the metal contacts (source and drain electrodes) positioned at the border of the device for experimental convenience. Layer B, which comprises super-hydrophobic SU8 micro pillars arranged to form a square pattern, in which the spacing of the pillars is not constant over the domain and this permits the automatic overlap of the solution droplet with the center of the device. A certain number of pillars (here, 5) is further modified to incorporate micro-electrodes in a line on the device for measurements of charged ions in a solution. The entire substrate is then spin coated with a conductive PEDOT:PSS thin film. A fluorocarbon polymer (C_4F_8) is finally deposited on the devices to assure hydrophobicity [22]. We used P-doped, (100) silicon wafers with an intermediate 5–10 Ohm/cm resistivity as substrates; before use, they were cleaned with acetone and isopropanol and then etched with a 4% hydrofluoric acid (HF) solution. Finally, the substrates were rinsed with DI water and dried with nitrogen flux.

Microfabrication of gold conductive patterns on the supporting silicon substrates (Layer A). Standard optical lithography techniques (Suss Microtec MA6/BA6, Sunnyvale, CA, USA) were employed to generate patterns of the circuits within a layer of positive tone resist (S1813) that was spin-coated onto clean silicon wafers. The masks necessary for optical lithography were fabricated using direct SEM (Scanning Electron Microscope) lithography**.** Upon evaporation of a 70 nm layer of gold on the sample, a lift-off process in an excesses of acetone was used to remove the un-exposed resist from the substrate, and define the pattern of gold circuits.

Microfabrication of Patterned Super-hydrophobic Surfaces (Layer B). A non-periodic pattern of super-hydrophobic micro pillars was realized on the substrate. We followed the methods described in[15] to modify the pattern of pillars from originally squared to a lattice in which the distance δ between the pillars transitions from the border to the center of the lattice with a power law of the distance. In what follows, the diameter and height of the pillars is adjusted to d=10 μm and h=20 μm respectively. A similar non-uniform distribution of pillars results in turn into a variable surface energy density that varies on the surface with the distance from the center of the pattern and in that center reaches a minimum. We obtained patterns of SU8-25 pillars with the described geometry on the substrate using standard optical lithography techniques. Direct laser writing (Heidelberg DWL 66fs) was used to fabricate the masks necessary for optical lithography. The correct alignment of layer A with layer B was assured by alignment markers positioned at the margins of the patterns.

Realizing Micro-Electrodes on the Top of the Pillars. Some pillars were further modified to incorporate metallic contacts which connect the described pillars to the gold contact area, using EBID (Electron Beam-Induced Deposition) fabrication. This process consists in injecting a precursor gas including Pt-C into the SEM chamber; the gaseous molecules are then hit by the electron beam and precipitate onto the substrate with a high spatial accuracy. A SEM column current of 1.6 nA and voltage 20 kV are set and these permit to deposit a layer of platinum approximately 100 nm thick. In the process, a dwell time of 200 ns and a thickness parameter of 15 μm are set.

The Conductive PEDOT:PSS Thin Film. The conductive PEDOT:PSS polymer (H.C. Starck-Clevios PH500), was finally spun onto the samples. PEDOT:PSS solution was previously doped with ethylene glycol (Sigma Aldrich) to enhance its electrical conductivity and dodecyl benzene sulfonic acid (DBSA) surfactant (Sigma Aldrich) to improve film forming. After deposition, samples were

baked at 140° C for 1 h. Finally, the device was completed with the deposition of a thin film of C_4F_8 to assure hydrophobicity [22].

SEM Characterization. SEM micrographs of the samples were acquired using a Dual Beam (SEM-FIB) - FEI Nova 600 NanoLab system. In measuring the pattern of SU8 polymeric pillars, we used a moderate 5 keV energy and corresponding electron current of 0.98 pA.

Contact angle characterization. We determined surface hydrophobicity of the samples by measuring the contact angle of a drop (approximately 5 μl in volume) of DI water gently positioned on the substrate with an automatic contact angle meter (KSV CAM 101, KSV Instruments LTD, Helsinki, Finland). Measurements were performed from 5 to 10 s after deposition.

Measuring the electrical activity of species in solution. Analytes in diluted solutions were positioned on the surfaces. The electrical activity of the device was measured using a 2-channel source/measure precision unit (Agilent B2902A) similarly to other reported experiments [5]. Gold metal thin film have been contacted through high precision metallic tips. Each chip contains 5 active points in a line and every measurements have been made contacting only one point at time. The two gold electrode were contacted on each side, in such a way to let the current go through the active PEDOT:PSS channel between the contacts, which represents source and drain in the transistor architecture. The contacts reach the top of one pillar and the active channel in between results in contact with the liquid drop on the pillars. The drop of electrolyte has been suspended over the pillars, on top of the contacts on the surface in the central part of the chip. Ag/Pt wires are immersed into the electrolyte drop, acting as gate electrode. The drain voltage Vds induces hole drifting in the channel and generates the channel current Ids. Upon application of a positive gate potential Vgs, cations are transported from the electrolyte to the PEDOT:PSS channel [14] and a dedoping process is initiated. Biosensor current response is expressed as current modulation $\Delta I/I_o = (I - I_o)/I_o$, where I is the drain current value measured for Vgs > 0 V and I_o is the Ids value for Vgs=0 V.

Solute distribution within the droplet. The distribution of a trace in a slowly evaporating droplet was derived on solving the Langevin equation [23-25]

$$m\frac{\partial \boldsymbol{u}}{\partial t} = 6\pi\mu a\left(K_p\boldsymbol{u} - K_f\boldsymbol{v}\right) + \mathbf{F}_E + \mathbf{F}_B \qquad (1)$$

where **u** is the unknown velocity vector for the particle, **v** is the unperturbed fluid velocity, a is the particle radius, and m is the particle mass. The first term on the right-hand side of Eq.(1) represents

the hydrodynamic drag on the particle. In Eq.(1), $\mathbf{F}_E = zeE_x\,\boldsymbol{e}_x$ represents the electrostatic force that is exerted by the externally applied Electric field, while $|\mathbf{F}_B| = \varsigma\sqrt{12\pi a\mu K_b T/\Delta t}$ is the Brownian force. Moreover: z is the charge number, $e{\sim}1.6\ 10^{-19}\ C$ is the elementary charge, $E_x = -\partial V/\partial x \sim 100\ V/m$ is the electric field that here has the longitudinal component solely and is derived starting from the applied voltage V, assuming that V varies linearly along the droplet; ς is a Gaussian number with zero mean and unit variance; $\mu = 10^{-3}\ Pa\ s$ is the viscosity of water; $T = 298\ K$ is the temperature of the system; Δt is the discrete time step of the simulation specified below. K_p and K_f are diagonal matrices describing the additional hydrodynamic hindrance associated with interactions between the particle and the system boundaries are here set equal to zero. For the unperturbed fluid velocity we used the solution provided by Tam and colleagues[21], who developed an analytical solution to the thermo-capillary driven Marangoni flow in a small droplet of water sitting on a super-hydrophobic surface in terms of stream-functions. Equation (1) was solved using a numerical scheme. The simulations are forward Euler integrations of the finite-difference equations resulting from discretization of the diffusion and convective operators as in[26, 27].

Results

Arrays of SU8 micro-pillars were fabricated using the techniques described in the Methods. The described pillars form a non-periodic lattice in which the pillar to pillar distance δ smoothly transitions from the periphery ($\delta = 30\ \mu m$) to the center O ($\delta{\sim}11\ \mu m$) of the lattice, and this would generate an energy minimum [15] and in turn a system of surface forces that recalls and confines the drop in O (Figure 1b, Figure 2a). A certain number of pillars (here, 5) is further modified to incorporate micro-electrodes in a line (Figure 2b). Each electrode is a system of two facing gold parallelepipeds in which the dimensional scale of the electrode is controlled in the low micro-meter range and the small gap between the parallelepipeds generates high density and localized electric fields. The modified pillars represent the active spots of the device which measure the electric activity of the target species in specific points of the solution. This permits to resolve the measurements in space. The correct alignment between the drop and the substrate ensures repeatability and reproducibility of the measurements. The entire system is coated with a conductive PEDOT:PSS polymer and in cascade with a (C_4F_8) fluorocarbon polymer which assures the hydrophobicity of the device with contact angles as large as large as 165° (Figure 2c).

When a drop a solution is deposited on the super-hydrophobic substrate, it maintains a quasi-spherical shape, with a strong curvature that is roughly equal to the reciprocal of its radius prior deposition. Because of its curvature, the drop develops convective flows within its volume and these are described by the celebrated Marangoni effect [19]. A molecule in the drop would be displaced by convection forces that are proportional to its cross section [21], and by diffusion forces that are proportional to the reciprocal of the cross section of the molecule [28]. The movement of a species in drop would be conditional to the steric radius of the species and species with different radii would present different trajectories. Computer simulations (see Methods) show the distribution of an ensemble of 500 particles in a spherical drop $2 \times 10^{-3}\ s$ post injection for a small ($radius = 0.02\ nm$) and a large ($radius = 2\ nm$) particle radius. In what follows, we adopt rectangular coordinates and an xy frame of reference in which the x coordinate is directed towards the substrate (that is, the drop is rotated by 90 degrees with respect to the horizon). While initially the particles are scattered randomly in the drop (Figure 3a), at the final time of flight they are preferentially distributed either at the center of the substrate for the large radius configuration (Figure 3b) or at the border of the substrate for the small radius configuration (Figure 3c). The competition between convection and diffusion in the drop is responsible for the different particle distribution. This difference may be at the basis of the separation of molecules in a mixture depending on molecule size.

The device was used to detect and separate biomolecules in solution, that are (i) cetyl trimethylammonium bromide (CTAB) and (ii) adrenaline. CTAB and adrenaline were used here in a concentration of $C = 10^{-5}\ M$. The primary interest of the presented research is demonstrating species separation more than detection in low abundance ranges. Future work will focus on finding molecules in lower ranges down to femto ($10^{-15}\ M$) to apto ($10^{-18}\ M$) molar. Transistor architecture of OECTs and associated high signal to noise ratio make this a realistic goal. As a comparison, current practice pushes the limits of detection for adrenaline to $10^{-7}\ M$[29].

CTAB is an organic compound with a positive net charge $z = 1$ and a diffusion coefficient $D^{CTAB} \sim 10^{-10}\ m^2/s$, from which its Stokes radius a^{CTAB} may be estimated being $a^{CTAB} = K_b T / 6\pi\mu\, D^{CTAB} \sim 2.18\ nm$. Depending on the concentration, CTAB monomers may cluster together to form supramolecular aggregates of those monomers[12] (micelles). In this form, they are of primary interest in drug delivery because of the potential use as drug carriers[30]. Adrenaline is a functional neurotransmitter. The net charge of adrenaline averaged over its

structure is $z = 1$. Moreover its *equivalent* diffusion coefficient is $D^{ad} \sim 93 \times 10^{-10}\ m^2/s$ and thus $a^{ad} \sim 0.023\ nm$. Adrenaline plays a central role in many instinctive responses, especially under stress situations and strongly physical strengthens. A timely sensing of abnormal adrenaline concentration could be an indicator of a pathological situation, like panic or heart attack, or could identify a typical flight, fight and fright response[31].

In Figure 4a we report the maximum drain-source current I_M for CTAB and adrenaline, individually placed in solution, as a function of micro electrode number and thus position on the device; in the figure, the values are presented for a fixed gate voltage $V_{gs} = 1\ V$ and are renormalized with respect to the unperturbed current I_{dso}. On analyzing the diagrams, one may observe that I_M depends on the position of the active micro-electrode on the substrate. Small adrenaline molecules are preferentially transported to the periphery of the device. Differently, the distribution of large CTAB molecules is uniform over the considered range of points. This confirms the results presented in Figure 3 and comments thereof. The discrepancy between adrenaline and CTAB may be ascribed to the sole difference in mass between those species.

Consider now the combination of CTAB and adrenaline. The device still measures a response that is space dependent (this is the trace named *difference* in Figure 4a), and thus the device captures a space-dependent distribution of the mixture. We can retrieve the relative content of CTAB and adrenaline in different points of the device using the time evolution of the signal as in Figure 4b. Here, adrenaline smoothly transitions from a minimum to a maximum, compared to the time response of CTAB that resembles a flat response typical of a second order system. Using the information contained in Figure 4b, the derivative of the time response of a mixture of CTAB and adrenaline (data not shown) may be decomposed in simpler components as in a linear LU decomposition and the coefficients extracted therefrom represent the relative content of CTAB and adrenaline in the mixture. For this particular configuration, we obtained obtain $\chi_{\#1}^{CTAB} = 0.31$, $\chi_{\#2}^{CTAB} = 0.520$, $\chi_{\#3}^{CTAB} = 0.713$, $\chi_{\#4}^{CTAB} = 0.458$, $\chi_{\#5}^{CTAB} = 0.281$, ($\chi^{ad} = 1 - \chi^{CTAB}$) and thus CTAB is transported preferentially at the internal of the pattern.

Conclusions

Here, we used in combination an OECT with a super-hydrophobic scheme to obtain substrates in which a finite number of points is independently controlled for site specific measurements of

electric-active solutions. In analyzing the current trace of different species in solution, we observed that the time evolution of those species would depend on the charge q and the coefficient of diffusion D of the ions, and on the Marangoni flow developed within the solution. The competition between convection and diffusion would cause a separation of species in the domain. The capability of resolving the trace of those ion-dependent signals either in space and in time, permits to the device to operate the separation of different species, based on their size and charge, similarly to a molecular filter, in which the mesh of the filter is not a material pattern but a physical process. This concept may have major applications in biology, medicine, biomedicine, for the detection of multiple species extracted from serum or other biological fluids. In cancer research, a similar device may separate from an un-informative waste deposit specific biological markers which indicate the outcome, progress, or both, of a disease, or the susceptibility of the disease to a given treatment. The identification of the content of a solution and information thereof may be operated by not trained or minimally trained personnel, and this information may help physicians in evaluating of the health status of patients or ongoing patient assessment, with major beneficial consequences for the national health care.

Figure Captions

Figure 1 Schematic of the device, in which a solution in form of a drop is automatically centered on the substrate; electrodes are integrated on the surface to permit space resolved measurements of the solution (a); the electrodes are connected to five pillars in a line contained in the region of the pattern in which the inter-pillar distance is variable, as in (b).

Figure 2 SEM image of the device, in which the electrodes runs through the substrate to realize a series of five measurement points in a line, also, one may notice the smoothly variable pattern of pillars which recalls a drop of solution at the center of the device (a); individual pillars (here, 5) are modified to incorporate micro-electrodes, which represent the active or sensitive spots of the device (b). The entire system is coated with a conductive PEDOT:PSS polymer and in cascade with a (C_4F_8) fluorocarbon polymer which assures the hydrophobicity of the device (c).

Figure 3 Simulations reveal the pattern of a bolus of 500 particles in a drop caused by diffusion and convection. The movement of the particles would depend on the size of the dislodging particles and species with different radii would present different trajectories. Initially the

particles are uniformly distributed in the drop (a). 2 ms post injection, the particles accumulate at the center of the substrate for the large radius configuration ($radius = 2\ nm$, b), and at the border of the substrate for the for the small radius configuration ($radius = 0.02\ nm$, c).

Figure 4 The modulation (maximum drain-source current) as a function of the position on the device (micro-electrode number) for the sole CTAB, for the sole adrenaline, and a combination of the two; the difference between adrenaline and CTAB may be ascribed to the difference in mass (and thus size) between these species (a). The difference between adrenaline and CTAB is reflected by the time evolution of the signal associated to these species: adrenaline smoothly transitions from a minimum to a maximum, compared to the time response of CTAB that resembles a flat response typical of a second order system (b).

Acknowledgments

This work has been partially funded from the Italian Minister of Health (Project n. GR-2010-2320665). NC acknowledges Nicola Zambelli and Giacomo Benassi for technical support.

References

[1] C.D. Dimitrakopoulos, P.R.L. Malenfant, Organic Thin Film Transistors for Large Area Electronics, Advanced Materials, 14 (2002) 99–117.

[2] R.M. Owens, G.G. Malliaras, Organic Electronics at the Interface with Biology, MRS Bulletin, 35 (2010) 449-456.

[3] G. Tarabella, C. Santato, S.Y. Yang, S. Iannotta, G.G. Malliaras, F. Cicoira, Effect of the gate electrode on the response of organic electrochemical transistors, Applied Physics Letters, 97 (2010) 123304.

[4] D. Khodagholy, T. Doublet, P. Quilichini, M. Gurfinkel, P. Leleux, A. Ghestem, E. Ismailova, T. Hervé, S. Sanaur, C. Bernard, G.G. Malliaras, In vivo recordings of brain activity using organic transistors, Nature Communications, 4 (2013) 1-7.

[5] F. Gentile, N. Coppedè, G. Tarabella, M. Villani, D. Calestani, P. Candeloro, S. Iannotta, E. Di Fabrizio, Microtexturing of the Conductive PEDOT:PSS Polymer for Superhydrophobic Organic Electrochemical Transistors, BioMed Research International, (2014) 1-10.

[6] P. Lin, X.T. Luo, I.M. Hsing, F. Yan, Organic Electrochemical Transistors Integrated in Flexible Microfluidic Systems and Used for Label-Free DNA Sensing, Advanced Materials, 23 (2011) 4035–4040.

[7] E.F. Petricoin, D.K. Ornstein, C.P. Paweletz, A. Ardekani, P.S. Hackett, B.A. Hitt, A. Velasco, C. Trucco, L. Wiegand, K. Wood, C.B. Simone, P.J. Levine, W.M. Linehan, M.R. Emmert-Buck, S.M. Steinberg, E.C. Kohn, L.A. Liotta, Serum Proteomic Patterns for Detection of Prostate Cancer, Journal of the National Cancer Institute, 94 (2002).

[8] P. Lin, F. Yan, J. Yu, H.L.W. Chan, M. Yang, The Application of Organic Electrochemical Transistors in Cell-Based Biosensors, Advanced Materials, 22 (2010) 3655–3660.

[9] G. Tarabella, A.G. Balducci, N. Coppedè, S. Marasso, P. D'Angelo, S. Barbieri, M. Cocuzza, P. Colombo, F. Sonvico, R. Mosca, S. Iannotta, Liposome sensing and monitoring by organic electrochemical transistors integrated in microfluidics, Biochimica et Biophysica Acta, 1830 (2013) 4374–4380.

[10] J.T. Mabeck, G.G. Malliaras, Chemical and Biological Sensors Based on Organic Thin-Film Transistors, Analytical and Bioanalytical Chemistry, 384 (2006) 343-353.

[11] E.C. Yusko, J.M. Johnson, S. Majd, P. Prangkio, R.C. Rollings, J. Li, J. Yang, M. Mayer, Controlling protein translocation through nanopores with bio-inspired fluid walls, Nature Nanotechnology, 6 (2011) 253-260.

[12] G. Tarabella, G. Nanda, M. Villani, N. Coppedè, R. Mosca, G.G. Malliaras, C. Santato, S. Iannotta, F. Cicoira, Organic electrochemical transistors monitoring micelle formation, Chemical Science, 3 (2012) 3432-3435.

[13] D.A. Bernards, G.G. Malliaras, Steady-State and Transient Behavior of Organic Electrochemical Transistors, Advanced Functional Materials, 17 (2007) 3538–3544.

[14] N. Coppedè, M. Villani, F. Gentile, Diffusion Driven Selectivity in Organic Electrochemical Transistors, Scientific Reports, 4 (2014) 1-7.

[15] F. Gentile, M.L. Coluccio, E. Rondanina, S. Santoriello, D. Di Mascolo, A. Accardo, M. Francardi, F. De Angelis, P. Candeloroa, E. Di Fabrizio, Non periodic patterning of super-hydrophobic surfaces for the manipulation of few molecules, Microelectronic Engineering, 111 (2013) 272-276.

[16] F. Gentile, M. Coluccio, N. Coppedè, F. Mecarini, G. Das, C. Liberale, L. Tirinato, M. Leoncini, G. Perozziello, P. Candeloro, F. De Angelis, E. Di Fabrizio, Superhydrophobic Surfaces as Smart Platforms for the Analysis of Diluted Biological Solutions, ACS Applied Materials and Interfaces, 4 (2012) 3213–3224.

[17] R. Blossey, Self-cleaning surfaces - virtual realities, Nature Materials, 2 (2003) 301-306.

[18] A. Lafuma, D. Quéré, Superhydrophobic states, Nature Materials, 2 (2003) 457-460.

[19] R.D. Deegan, O. Bakajin, T.F. Dupont, G. Huber, S.R. Nagel, T.A. Witten, Capillary flow as the cause of ring stains from dried liquid drops, Nature, 389 (1997) 827-829.

[20] H. Masoud, J.D. Felske, Analytical solution of Stokes flow inside an evaporating sessile drop: Spherical and cylindrical cap shapes, Physics of Fluids, 21 (2009) 042102.

[21] D. Tam, V. von Arnim, G.H. McKinley, A.E. Hosoi, Marangoni convection in droplets on superhydrophobic surfaces, Journal of Fluid Mechanics, 624 (2009) 101- 123.

[22] T. Limongi, F. Cesca, F. Gentile, R. Marotta, R. Ruffilli, A. Barberis, M.D. Maschio, E.M. Petrini, S. Santoriello, F. Benfenati, E. Di Fabrizio, Nanostructured Superhydrophobic Substrates Trigger the Development of 3D Neuronal Networks, Small, 9 (2013) 402–412.

[23] Y. Astier, L. Data, R.P. Carney, F. Stellacci, F. Gentile, E. Di Fabrizio, Artificial Surface-Modified Si3N4 Nanopores for Single Surface-Modified Gold Nanoparticle Scanning, Small, 7 (2010) 455-459.

[24] M.-m. Kim, A.L. Zydney, Effect of electrostatic, hydrodynamic, and Brownian forces on particle trajectories and sieving in normal flow filtration, Journal of Colloid and Interface Science, 269 (2004) 425–431.

[25] F. Gentile, M.L. Coluccio, R.P. Zaccaria, M. Francardi, G. Cojoc, G. Perozziello, R. Raimondo, P. Candeloroa, E.D. Fabrizio, Selective on site separation and detection of molecules in diluted solutions with superhydrophobic clusters of plasmonic nanoparticles, Nanoscale, 6 (2014) 8208-8225.

[26] D. Dubin, Numerical and Analytical Methods for Scientists and Engineering Using Mathematica, John Wiley & Sons, Hoboken, 2003.

[27] J.E. Pearson, Complex Patterns in a Simple System, Science, 261 (1993) 189-192.

[28] F. Gentile, M. Ferrari, P. Decuzzi, The transport of nanoparticles in blood vessels: The effect of vessel permeability and blood rheology, Annals of Biomedical Engineering, 2 (2008) 254–261.

[29] X. Zhou, J. Huang, M. Li, B. Wang, A novel method of adrenaline concentration detection using fiber optical biosensor based on the catalysis of iron(II) phthalocyanine, proceedings of SPIE, 7278 (2012) 1-4.

[30] G. Verma, P.A. Hassan, Self assembled materials: design strategies and drug delivery perspectives, Phys Chem Chem Phys, 15 (2013) 17016-17028.

[31] N. Coppedè, G. Tarabella, M. Villani, D. Calestani, S. Iannotta, A. Zappettinia, Human Stress Monitoring Through an Organic Cotton-Fiber Biosensor, Journal of Materials Chemistry B, 2 (2014) 5620-5626.

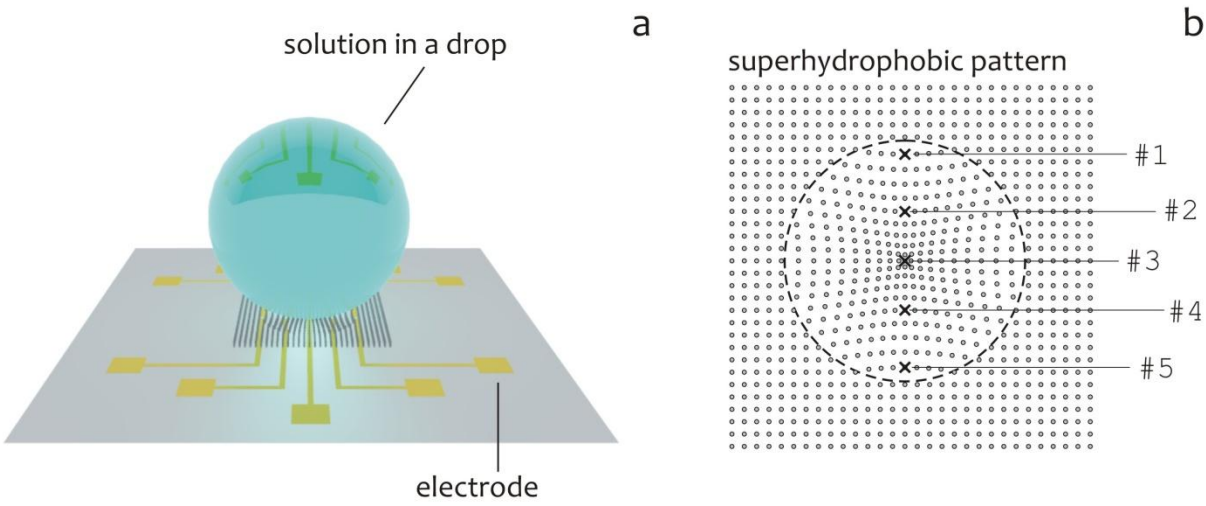

Figure 1

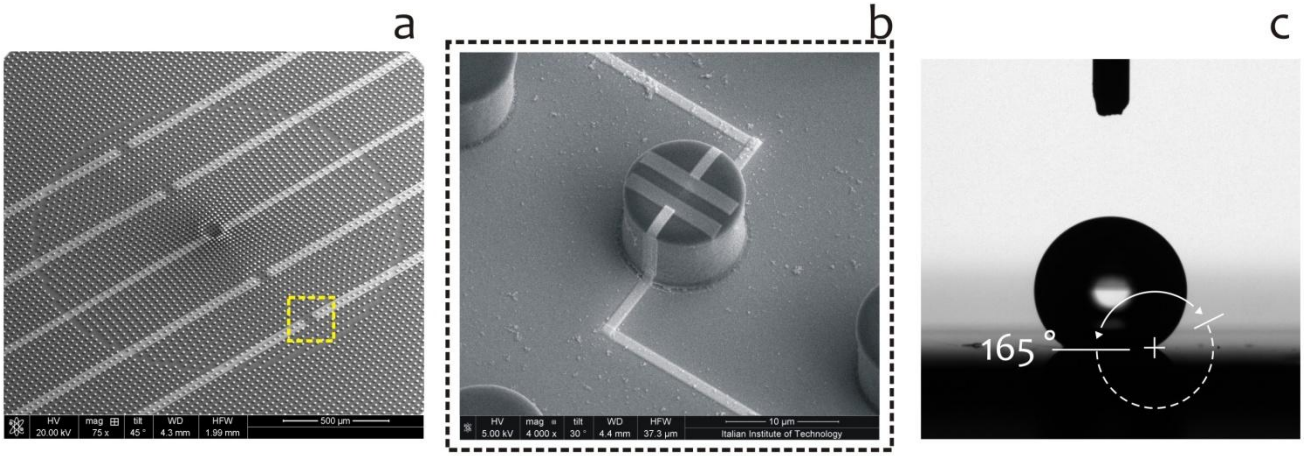

Figure 2

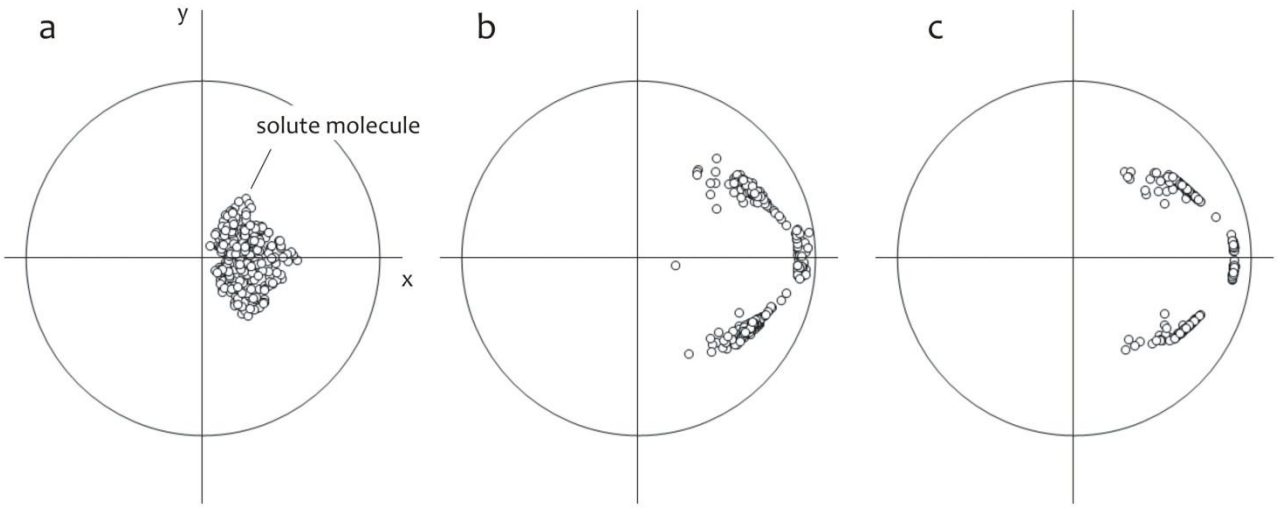

Figure 3

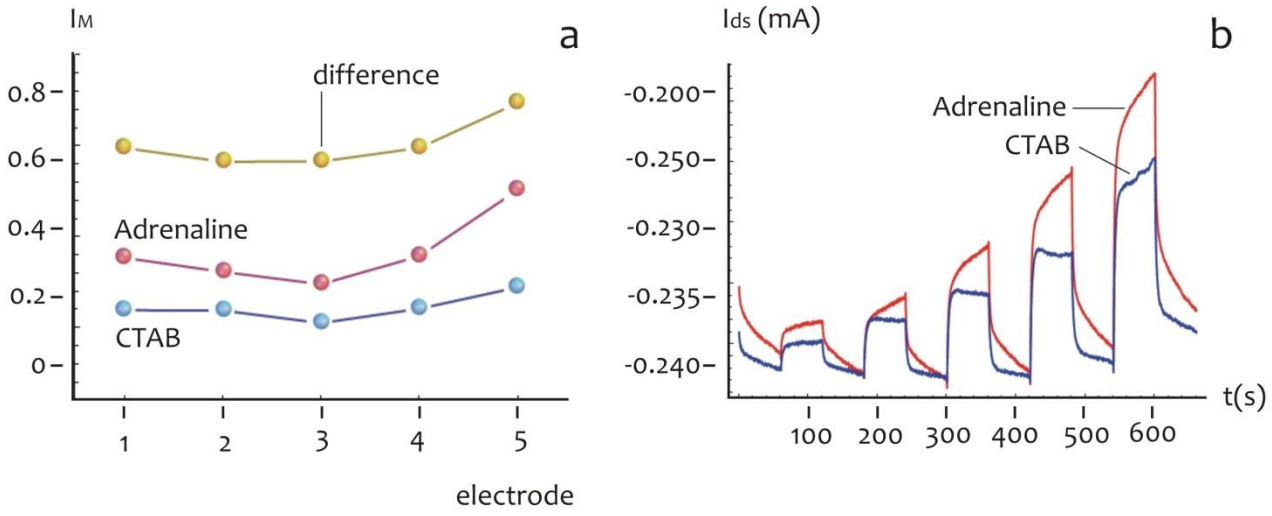

Figure 4

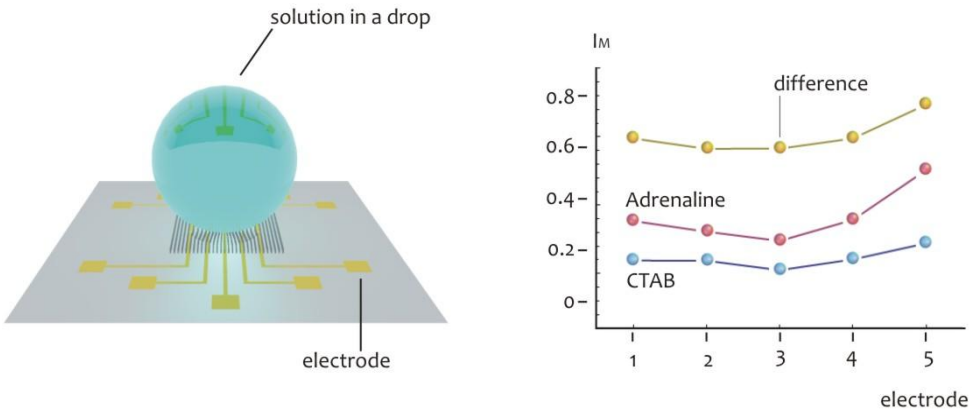

Graphical abstract

Highlights

- We combine a conductive PEODOT:PSS polymer with a super-hydrophobic scheme
- We fabricate OECT devices for time and space resolved analysis of a solution
- Convection and diffusion in the drop separate species based on their size and charge
- Our device delivers the ability to register a similar difference
- We demonstrate the device in the detection of a mixture of CTAB and adrenaline